Vacuum 72 (2004) 241–248

Structure, hardness and thermal stability of nanolayered TiN/CrN multilayer coatings

Harish C. Barshilia[a,*], Anjana Jain[b], K.S. Rajam[a]

[a] *Surface Engineering Division, National Aerospace Laboratories, Post Bag No. 1779, Bangalore 560 017, India*
[b] *Materials Science Division, National Aerospace Laboratories, Post Bag No. 1779, Bangalore 560 017, India*

Received 21 May 2003; received in revised form 5 August 2003; accepted 5 August 2003

Abstract

Nanolayered TiN/CrN multilayer coatings were deposited on silicon substrates using a reactive DC magnetron sputtering process at various modulation wavelengths (Λ), substrate biases (V_B) and substrate temperatures (T_S). X-ray diffraction (XRD), nanoindentation and atomic force microscopy (AFM) were used to characterize the coatings. The XRD confirmed the formation of superlattice structure at low modulation wavelengths. The maximum hardness of the TiN/CrN multilayers was 3800 kg/mm^2 at $\Lambda = 80$ Å, $V_B = -150$ V and $T_S = 400$°C. Thermal stability of TiN, CrN and TiN/CrN multilayer coatings was studied by heating the coatings in air in the temperature range (T_A) of 400–800°C. The XRD data revealed that TiN/CrN multilayers retained superlattice structure even up to 700°C and oxides were detected only after $T_A \geqslant 750$°C, whereas for single layer TiN and CrN coatings oxides were detected even at 550°C and 600°C, respectively. Nanoindentation measurements showed that TiN/CrN multilayers retained a hardness of 2800 kg/mm^2 upon annealing at 700°C, and this decrease in the hardness was attributed to interdiffusion at the interfaces.

Keywords: TiN/CrN multilayers; Reactive DC magnetron sputtering; X-ray diffraction; Nanoindentation; Thermal stability

1. Introduction

A variety of nanolayered multilayer coatings, also known as superlattices, have been studied extensively in recent years because of their promising properties [1,2]. Multilayer coatings of ceramic materials are an emerging class of hard materials. The properties of the superlattices depend critically on the modulation wavelength (Λ), that is the bilayer thickness. The ceramic superlattices exhibit exotic mechanical properties. For example, a hardness of greater than 5000 kg/mm^2 has been reported for single-crystalline TiN/NbN and TiN/VN superlattices with a modulation wavelength of 50–85 Å [3,4]. Apart from high hardness, the ceramic multilayer coatings also exhibit high strength, and wear resistance [5,6]. Therefore, these coatings have great potential as protective coatings on cutting tools and other mechanical components. For cutting tool applications one not only needs to prepare hard and

*Corresponding author. Tel.: +91-805086494; fax: +91-805210113.
E-mail address: harish@css.cmmacs.ernet.in (H.C. Barshilia).

0042-207X/$ - see front matter © 2003 Elsevier Ltd. All rights reserved.
doi:10.1016/j.vacuum.2003.08.003

tough coatings but their thermal stability is also very important. Tools protected by the hard coatings often operate at elevated temperatures in air. The thermal stability of TiN and CrN coatings has been studied in the literature [7–12]. Though TiN is harder than CrN it suffers from lower thermal stability. CrN has been reported to be more thermally stable than TiN [8,12]. TiN/CrN multilayers are technologically important coatings and are expected to have superior mechanical and tribological properties [13–16]. Very few studies are reported on the thermal stability of nanolayered TiN/CrN multilayer superlattice coatings [17,18]. Also, the mechanical properties of TiN/CrN multilayers as a function of annealing temperature have not been studied in detail. The objectives of this paper are to study the structural and mechanical properties of TiN/CrN multilayers and also to discuss the thermal stability of these coatings.

2. Experimental details

Alternate layers of TiN and CrN of varying thicknesses were deposited on silicon (1 0 0) substrates using a reactive DC magnetron sputtering system. In order to get varying thicknesses of TiN and CrN layers, 3″ diameter high purity Ti (99.95%) and Cr (99.99%) targets were sputtered for different durations in high purity argon (99.999%) and nitrogen (99.999%) plasma. The power densities were ~ 5 and $\sim 2\,W/cm^2$ for Ti and Cr targets, respectively. The Ti and Cr sputtering guns were shielded from each other to minimize the cross-contamination. Typically, TiN/CrN multilayers were deposited under a base pressure of $\sim 5.0 \times 10^{-4}$ Pa and a total $Ar + N_2$ gas pressure of $\sim 5.0 \times 10^{-1}$ Pa. Special gas feeding system was designed to create differential partial pressures of the reactive gas near the Cr and Ti targets as the heats of formation of TiN (80.8 kcal/mol) and CrN (29.8 kcal/mol) differ considerably. A total nitrogen flow rate of 2.0 sccm was used for all the depositions. A substrate bias varying from -50 to -250 V was applied to improve the mechanical properties of the coatings. An external radiant heater was used to heat the substrates during the deposition. A chromel–alumel thermocouple fixed near the substrate measured the substrate temperature. The substrates were chemically cleaned in an ultrasonic agitator in acetone, absolute alcohol and trichloroethylene. Subsequently, the substrates were cleaned in situ by Ar^+ ion bombardment for 30 min, wherein a DC bias of -850 V was applied to the substrate at an argon pressure of 6.0×10^{-1} Pa. A 0.5 μm thick Ti interlayer was deposited for all the samples to improve the adhesion of the coatings. Under these conditions, typical growth rates were ~ 2 and ~ 6 Å/s for TiN and CrN, respectively. The total thicknesses of the coatings were 2 μm. Multilayer coatings with controlled layer thicknesses and repeatability were deposited using a PC-based dwell time controller. In this system, a stepper motor was connected to the substrate holder through a rotary feedthrough. The stepper motor was controlled by a driver circuit.

The X-ray diffraction (XRD) data of the coatings in Bragg–Brentano ($\theta-2\theta$) geometry were recorded in a Rigaku D/max 2200 Ultima X-ray powder diffractometer. The X-ray source was a Cu Kα radiation ($\lambda = 1.5418$ Å). The hardness measurements were performed in a nanoindenter (CSEM Instruments) at a load of 5 mN using a Berkovich diamond indenter. At this load the indentation depth was much less than 1/10th of the coating thickness, thus eliminating the effect of substrate on the hardness measurements. Ten indentations were made on each sample and results presented herein represent the averages of 10 indentations. Surface morphologies of the coatings were measured by atomic force microscopy (AFM), which was operated in non-contact mode (Surface Imaging Systems). In order to test the thermal stability of the coatings, TiN, CrN and TiN/CrN multilayers were simultaneously heated in air in a resistive furnace at $T_A = 400$°C, 500°C, 550°C, 600°C, 700°C, 750°C and 800°C. Annealing involved increasing the temperature of the samples from room temperature to the desired temperature at a slow heating rate of 3°C/min and maintaining the desired temperature for 30 min. Subsequently, the samples were cooled down at a rate of 3°C/min. The structural changes and hardness of the coatings as a result of heating were measured using XRD and nanoindentation, respectively.

3. Results and discussion

3.1. Structure of TiN/CrN Multilayers

It is known that CrN exists in different phases (c-CrN and β-Cr_2N) and there is a limited range of nitrogen concentration wherein stoichiometric phases of TiN and CrN with B1 NaCl structure exist. The deposition conditions were, therefore, carefully optimized after a series of experiments involving variations of nitrogen partial pressure, target power, operating pressure and substrate bias. Typical deposition conditions for TiN were: sputtering power = 225 W, substrate bias = −200 V, current density on the substrate = 1.1 mA/cm^2, total flow rate of nitrogen = 2.0 sccm and operating pressure = 4.0×10^{-1} Pa. CrN was deposited under the following conditions: sputtering power = 100 W, substrate bias = −200 V, current density on the substrate = 0.3 mA/cm^2, total flow rate of nitrogen = 2.0 sccm and operating pressure = 4.0×10^{-1} Pa. The flow distribution of nitrogen was made in such a way that higher partial pressure of nitrogen was created near Cr target than Ti target. Under these conditions cubic phases of TiN and CrN with {1 1 1} texture were obtained (results not presented). The intensity of (2 0 0) reflection for both TiN and CrN was low and other reflections such as (2 2 0) and (3 1 1) were not detected in the diffraction patterns. This showed that under these deposition conditions both TiN and CrN coatings had {1 1 1} texture.

After optimizing the deposition conditions for TiN and CrN, multilayer coatings were prepared at different modulation wavelengths, substrate temperatures and substrate biases. Fig. 1 shows typical XRD data of TiN/CrN multilayers deposited at four modulation wavelengths. The substrate bias was −200 V and the substrate temperature was 400°C. All the coatings exhibited first-order positive and negative satellite reflections (SR) along (1 1 1) principal reflection (PR), thus confirming the formation of superlattice structure. The first order satellite reflections were observed for 130 Å $\geqslant \Lambda \geqslant$ 40 Å. Coatings deposited at higher Λs showed even second-order satellite reflections. The peak centered at $2\theta = 40.1^\circ$ was assigned to Ti(0 1 1), which was from the titanium interlayer.

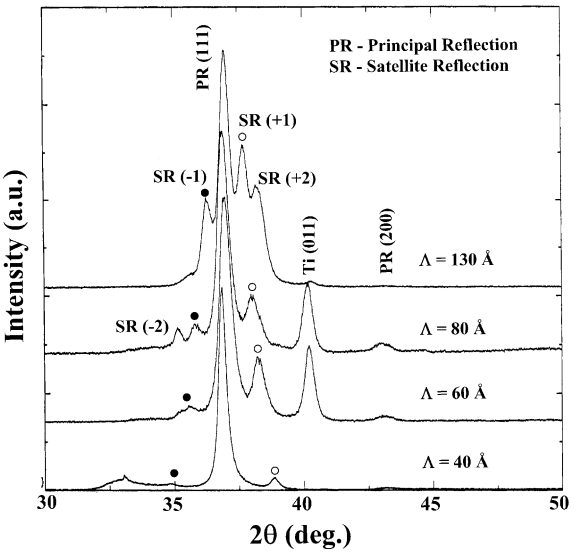

Fig. 1. High-angle XRD data of TiN/CrN multilayers deposited at different modulation wavelengths. The spectra show {1 1 1} texture and reveal satellite peaks on both sides of the main Bragg (1 1 1) reflection.

For the coating prepared at $\Lambda = 40$ Å an additional broad peak centered at $2\theta = 33.02^\circ$ was observed. This peak was due to impurities in the substrate, which was established by recording XRD data of the uncoated silicon substrate. For all the coatings the intensity of (2 0 0) principal reflection was very low as compared to the (1 1 1) principal reflection, indicating {1 1 1} texture of the coatings. The satellite peaks shifted towards principal reflection with an increase in the modulation wavelength. The intensity ratio of the satellite reflection to the main Bragg peak (I_S/I_B) decreased almost linearly with decreasing Λ, indicating that at low Λ the interfaces between CrN and TiN became diffused. As will be discussed later, coatings exhibited maximum hardness at $\Lambda = 80$ Å.

3.2. Hardness of TiN/CrN Multilayers

The hardness variation of TiN/CrN multilayers as a function of modulation wavelength is shown in Fig. 2. The substrate bias was −200 V and the substrate temperature was 400°C for all the

coatings. The measured hardnesses for CrN and TiN coatings deposited under the similar deposition conditions were $\sim$1000 and 2500 kg/mm^2, respectively. The rule-of-mixtures value would be $\sim$1750 kg/mm^2. In the modulation wavelength range 300 Å $\geqslant \Lambda \geqslant$ 40 Å, the hardness showed a peak at $\Lambda = 80$ Å and the maximum hardness was 3600 kg/mm^2. This enhancement in the hardness of multilayer coatings was about 2 times the rule-of-mixtures value. A variety of mechanisms have been put forward to explain the enhanced mechanical properties of the nanolayered multilayer coatings and these are discussed in the literature [19,20].

Apart from the modulation wavelength, hardness of the coatings was also dependent on the substrate bias and its variation is shown in Fig. 3. A maximum hardness of 3800 kg/mm^2 ($\Lambda = 80$ Å, $T_S = 400^\circ$C) was achieved at $V_B = -150$ V. The hardness decreased from 3800 to 1770 kg/mm^2 as the bias was decreased from -150 to -50 V. At higher substrate bias (e.g., $V_B \geqslant -200$ V) the hardness again decreased, presumably because of ion beam intermixing effects at the interfaces and interface roughening. This observation is consistent with the earlier reports on effect of substrate bias on the mechanical properties of multilayers

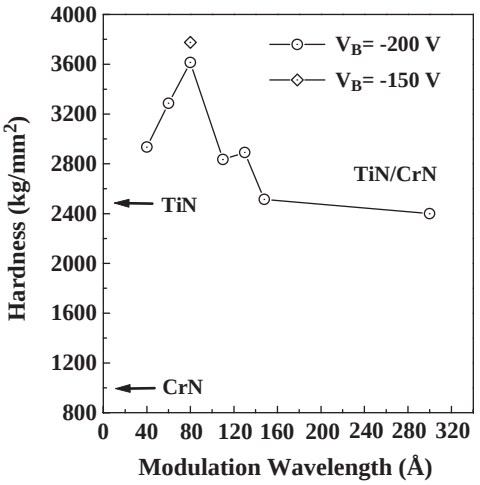

Fig. 2. Variation of nanoindentation hardness of TiN/CrN multilayer coatings with modulation wavelength. Also, shown are the hardnesses of single layer TiN and single layer CrN coatings.

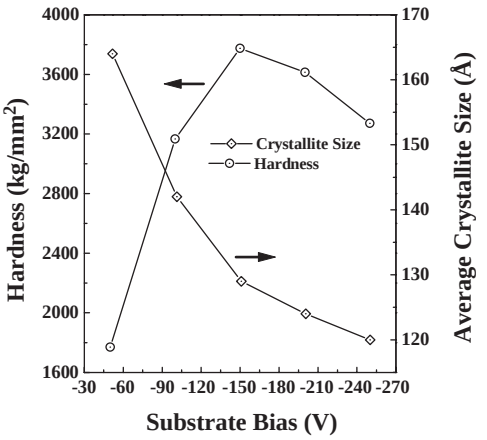

Fig. 3. Variation of nanoindentation hardness of TiN/CrN multilayer coatings with substrate bias. The modulation wavelength was 80 Å and the substrate temperature was 400°C. Also, shown is the variation of average crystallite size with substrate bias.

[21,22]. The enhanced hardness as a result of ion bombardment can be explained by ion-induced densification below -150 V and deterioration of the superlattice structure caused by interdiffusion and interface roughness above -150 V. Ion bombardment during the film growth suppresses the formation of the large grains with voided or cracked boundaries because of a continuous renucleation process. This was supported by XRD and AFM data. The average grain size, as determined from the Scherrer equation, decreased from 165 to 120 nm as the bias was increased from -50 to -250 V (see Fig. 3). The AFM images also showed fine-grained morphology for the coatings deposited at higher substrate bias voltages. Typical AFM images of 200 nm thick TiN/CrN multilayers ($\Lambda = 80$ Å, $T_S = 400^\circ$C) deposited at a substrate bias of -50 and -150 V are shown in Fig. 4. The decrease in the grain size with an increase in V_B has been reported for TiN coatings [23]. Increasing the substrate bias increases the energy of the impinging ions and as a result resputtering occurs. Furthermore, as the energy of the impinging ions increases, the generation of defects and preferential resputtering of ad-atoms increase, thus lowering the ad-atom mobility [24]. These processes, in turn, produce an increased number of preferential nucleation sites, which

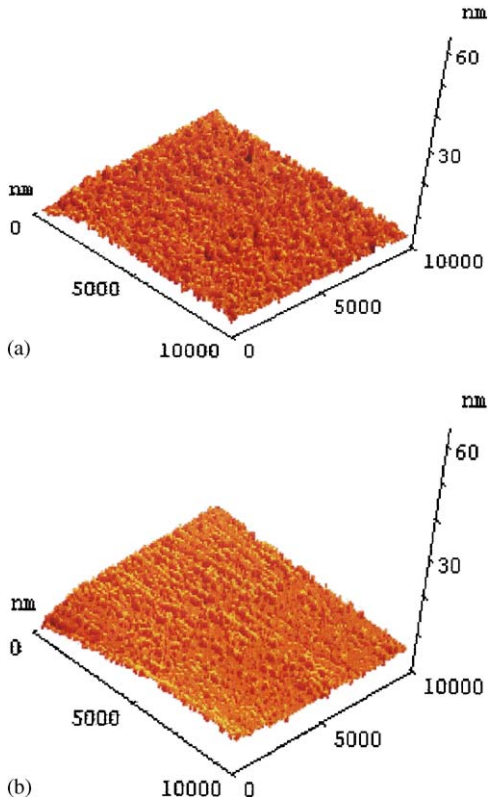

Fig. 4. (a) Three-dimensional AFM image of 200 nm thick TiN/CrN multilayer coating deposited at a substrate bias of −50 V. (b) Three-dimensional AFM image of 200 nm thick TiN/CrN multilayer coating deposited at a substrate bias of −150 V.

reduce the grain size [25]. The substrate bias affected the crystallite size but not the texture of the coatings. All the coatings showed {1 1 1} texture, irrespective of the substrate bias.

Another deposition parameter, which affected the hardness of TiN/CrN multilayer coatings was the substrate temperature. Films deposited at room temperature showed a hardness of $\sim 3000\,kg/mm^2$ ($\Lambda = 80$ Å, $V_B = -200$ V). With an increase in the substrate temperature up to 400°C the hardness increased gradually to $3600\,kg/mm^2$. Further increase in the substrate temperature up to 450°C resulted in marginal decrease in the hardness. The increased hardness of multilayer coatings with substrate temperature is believed to be due to reduced porosity of the coatings at higher deposition temperatures. Petrov et al. have reported a decrease in the intercolumnar porosity of TiN coatings with substrate temperature at a fixed substrate bias [23].

Moderately higher substrate temperature is also known to reduce the incorporation of argon atoms in the interstitial sites in sputtered coatings [26]. The decrease in the hardness for $T_S > 400$°C may be related to the interdiffusion between TiN and CrN layers, which increases the interface roughness and deteriorates the superlattice character of the coatings. Thus, an optimum substrate temperature of 400°C was used for all the multilayer depositions.

3.3. Thermal stability of TiN/CrN multilayers

Fig. 5 shows the XRD data of an as-deposited TiN/CrN multilayer coating and coatings heated in air at 700°C, 750°C and 800°C for 30 min. XRD patterns for samples heated at 400°C, 500°C and 600°C are not shown in Fig. 5 as no structural changes were observed for these samples. For all the coatings, the modulation wavelength was 80 Å, the substrate bias was −200 V, the substrate temperature was 400°C and the total thickness was 2 μm. TiN/CrN multilayer coating heat

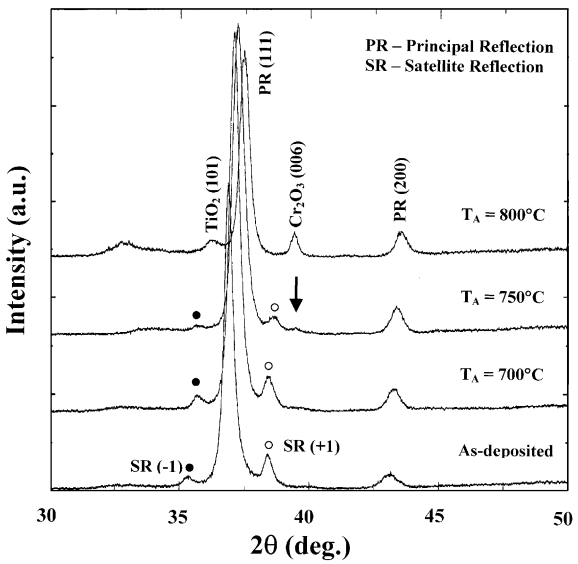

Fig. 5. High-angle XRD data of as-deposited TiN/CrN multilayer coating and coatings heated at 700°C, 750°C and 800°C. The modulation wavelength was 80 Å.

treated at 700°C showed satellite reflections along (1 1 1) principal reflection and no phases of titanium and chromium oxides were detected in the XRD data. Evolution of oxide phases was observed at $T_A = 750°C$ but the satellite peaks could still be seen at this temperature. However, the satellite peaks completely disappeared at 800°C. This indicated that coating retained its superlattice character even after heating up to 700°C. The main Bragg peak shifted to higher 2θ values with increasing T_A. This shift may be due to stress relaxation as a result of annealing. Compressive stresses are commonly observed in bias sputtered coatings because of defects created by Ar^+ ion bombardment [27]. Single layer coatings of CrN and TiN were also heated under identical conditions at 400°C, 500°C, 550°C, 600°C, 700°C, 750°C and 800°C. As shown in Fig. 6 for CrN coatings Cr_2O_3 was detected even at 600°C in the XRD. For $T_A \geqslant 700°C$ the coatings oxidized significantly. Similarly, TiO_2 was detected for TiN coatings at 550°C (results not shown).

For hard coatings it is important to study the mechanical properties at elevated temperatures, as these coatings are potential candidates for wear resistance applications in cutting tools. In Fig. 7 we plot the variation of hardness of TiN/CrN multilayer coatings ($\Lambda = 80$ Å, $T_S = 400°C$ and $V_B = -200$ V) as a function of annealing temperature. Nanoindentation data on coatings heated at 750°C and 800°C are not presented as these samples begun to oxidize and the measurements are expected to be incorrect. None of the TiN, CrN and multilayer coatings showed delamination as a result of heating even at the highest annealing temperature (800°C), indicating good adhesion between the coating and the substrate. It is interesting to note that even after annealing up to 700°C the multilayer coatings retained hardness as high as 2800 kg/mm^2. The decrease in the hardness of multilayer coatings as a result of annealing was attributed to interdiffusion at the interfaces. This was established by calculating the intensity ratio of satellite reflection to Bragg reflection in the XRD data, which is a measure of superlattice character [3]. Variations of I_S/I_B and hardness of multilayers with annealing temperature are shown in Fig. 8. Both hardness and (I_S/I_B) decreased almost linearly with T_A. The XRD and the nanoindentation data are, therefore, consistent with each other.

The oxidation mechanisms of TiN and CrN have been discussed in the literature. It has been reported that the oxidation of CrN is controlled by the

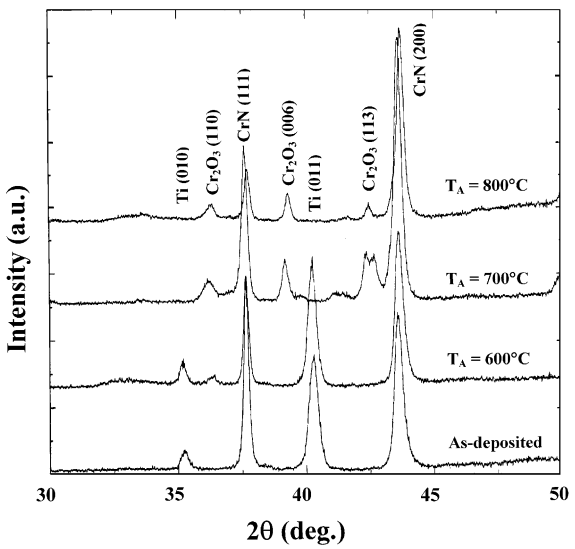

Fig. 6. High-angle XRD data of as-deposited CrN coating and coatings heated at 600°C, 700°C and 800°C.

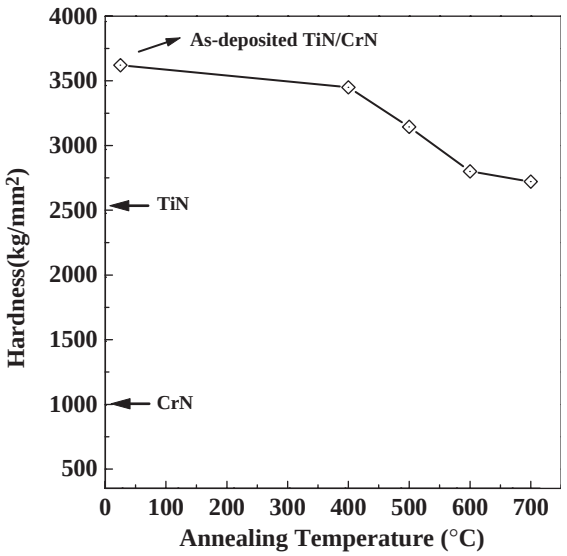

Fig. 7. Variation of hardness of TiN/CrN multilayers with annealing temperature.

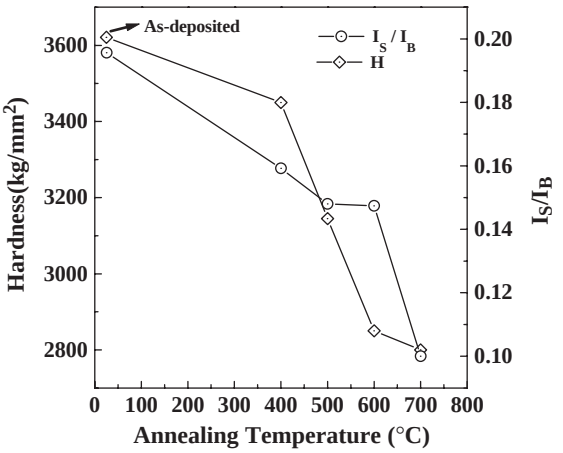

Fig. 8. Variations of hardness and normalized satellite reflection intensity of TiN/CrN multilayers with annealing temperature.

outward diffusion of Cr ions through the Cr_2O_3 layer formed on each CrN grain [8]. On the other hand, the oxidation of TiN is controlled by oxygen or nitrogen ion diffusion, which is enhanced by the grain boundaries of the formed oxide [7]. The grain size and recrystallization also affect the oxidation mechanism [28]. In multilayer coatings, presence of a large number of interfaces is expected to further affect the oxidation mechanism. Interdiffusion between the layers and different diffusion properties of O, N, Ti and Cr in TiN and CrN make the oxidation mechanism of TiN/CrN multilayers very complex. Clearly, a simple explanation for the enhanced thermal stability of multilayers is not feasible at this stage and further work is necessary.

The above results indicate that the primary limitations of TiN (lower thermal stability) and CrN (lower hardness) can be overcome by layering of the two materials on nanometer scale. Thus, the TiN/CrN multilayer coatings not only exhibit superior mechanical properties but also higher thermal stability as compared to the single layer TiN and CrN coatings.

4. Conclusions

TiN/CrN multilayer coatings were deposited on silicon substrates using a reactive DC magnetron sputtering process. The XRD data showed that coatings with modulation wavelength $130\,\text{Å} \geqslant \Lambda \geqslant 40\,\text{Å}$ exhibited a prominent principal reflection along (1 1 1) plane, which was flanked by first-order positive and negative satellite reflections, thus confirming the formation of a superlattice structure. TiN/CrN multilayer coatings showed a maximum hardness of 3800 kg/mm^2 at $\Lambda = 80$ Å, $V_B = -150$ V and $T_S = 400^\circ$C. The XRD data of heated TiN/CrN multilayers showed that the coatings retained superlattice structure even up to 700°C and oxide phases were detected only at $T_A \geqslant 750^\circ$C. Single layer TiN and CrN coatings begun to oxidize even at 550°C and 600°C, respectively. Nanoindentation measurements showed that the hardness of TiN/CrN multilayers decreased from 3600 to 2800 kg/mm^2 upon annealing at 700°C. This decrease in the hardness was attributed to interdiffusion at the interfaces.

Acknowledgements

The authors acknowledge the financial support provided by the Department of Science and Technology, New Delhi and the Council of Scientific and Industrial Research, New Delhi, India.

References

[1] Yashar PC, Sproul WD. Vacuum 1999;55:179.
[2] Barnett S, Madan A. Phys World 1998;45.
[3] Shinn M, Hultman L, Barnett SA. J Mater Res 1992;7:901.
[4] Helmersson U, Todorova S, Barnett SA, Sundgren JE, Markert LC, Greene JE. J Appl Phys 1987;62:481.
[5] Zhou YM, Asaki R, Higashi K, Soe WH, Yamamoto R. Surf Coat Tech 2000;130:9.
[6] Ljungcrantz H, Engstrom E, Hultman L, Olsson M, Chu X, Wong MS, Sproul WD. J Vac Sci Technol A 1998;16:3104.
[7] Ichimura H, Kawana A. J Mater Res 1993;8:1093.
[8] Ichimura H, Kawana A. J Mater Res 1994;9:151.
[9] Mayrhofer PH, Willmann H, Mitterer C. Surf Coat Tech 2001;146-147:222.
[10] Tu JN, Duh JG, Tsai SY. Surf Coat Tech 2000;133–134:181.
[11] Polyakova IG, Hubert T. Surf Coat Tech 2001;141:55.
[12] Milosev I, Strehblow HH, Navinsek B. Surf Coat Tech 1995;74-75:897.

[13] Nordin M, Larsson M, Hogmark S. Wear 1999;232:221.
[14] Zhou Y, Asaki R, Soe WH, Yamamoto R, Chen R, Iwabuchi A. Wear 1999;236:159.
[15] Yashar P, Barnett SA, Rechner J, Sproul WD. J Vac Technol A 1998;16:2913.
[16] Nordin M, Larsson M, Hogmark S. Surf Coat Tech 1998;106:234.
[17] Panjan P, Navinsek B, Cvelbar A, Zalar A, Vlcek J. Surf Coat Technol 1998;98:1497.
[18] Panjan P, Navinsek B, Cvelbar A, Zalar A, Milosev I. Thin Solid Films 1996;281-282:298.
[19] Barnett SA, Shinn M. Annu Rev Mater Sci 1994;24:481.
[20] Chu X, Barnett SA. J Appl Phys 1995;77:4403.
[21] Zeng XT. Surf Coat Tech 1999;113:75.
[22] Wong MS, Hsiao GY, Yang SY. Surf Coat Tech 2000; 133–134:160.
[23] Petrov I, Hultman L, Helmersson U, Sundgren JE, Greene JE. Thin Solid Films 1989;169:299.
[24] Sundgren JE. Thin Solid Films 1985;128:21.
[25] Sundgren JE, Johansson BO, Hentzell HTG, Karlsson SE. Thin Solid Films 1983;105:385.
[26] Vossen JL, Cuomo JJ. In: Vossen JL, Kern W, editors. Thin Film Processes. New York: Academic Press; 1978. p. 58.
[27] Ljungcrantz H, Hultman L, Sundgren JE, Karlsson L. J Appl Phys 1995;78:832.
[28] Andrievski RA, Anisimova IA, Anisimov VP, Makarov VP, Popova VP. Thin Solid Films 1995;261:83.